



Introduction to Neutron (and X-ray) Scattering Techniques

Jeffrey Lynn

NIST Center for Neutron Research

University of Texas—Dallas, Arlington
April 12, 2021



Outline

- Scattering Basics
 - Cross sections, form factors, x-rays vs. neutrons
- Powder Diffraction (crystal and magnetic diffraction)
 - Profile refinement, subtraction technique, polarized neutrons
- Single Crystal Diffraction (structure and magnetic)
- Small Angle Neutron Scattering (SANS)
 - Nanoparticles, Vortex lattice, ferromagnetic superconductor, skyrmions, domains, ... polymers, biological systems,
- Reflectometry (thin films and multilayers)
 - Structural and Magnetic Depth Profile
- Inelastic Scattering
 - Phonons, Magnons, Crystal Field Levels, Spin Liquids,
- Reference Materials

Neutron (and X-ray) scattering

NCNR

Neutron scattering experiments measure the flux of neutrons scattered by a sample into a detector as a function of the change in neutron wave vector (\vec{Q}) and energy ($\hbar\omega$).

Momentum

$$\hbar k_n = \hbar(2\pi/\lambda_n)$$

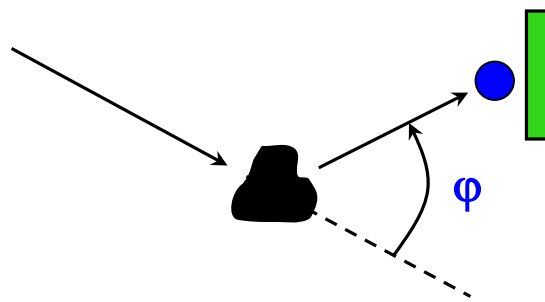
$$\hbar\vec{Q} = \hbar\vec{k}_i - \hbar\vec{k}_f$$

Energy

$$E = \hbar^2 k_n^2 / 2m$$

$$E = E_i - E_f$$

$$\Phi(Q, \hbar\omega) = \frac{\text{neutrons}}{\text{sec-cm}^2}$$



The expressions for the scattered neutron flux Φ depend on the positions and motions of atomic nuclei or unpaired electron spins.

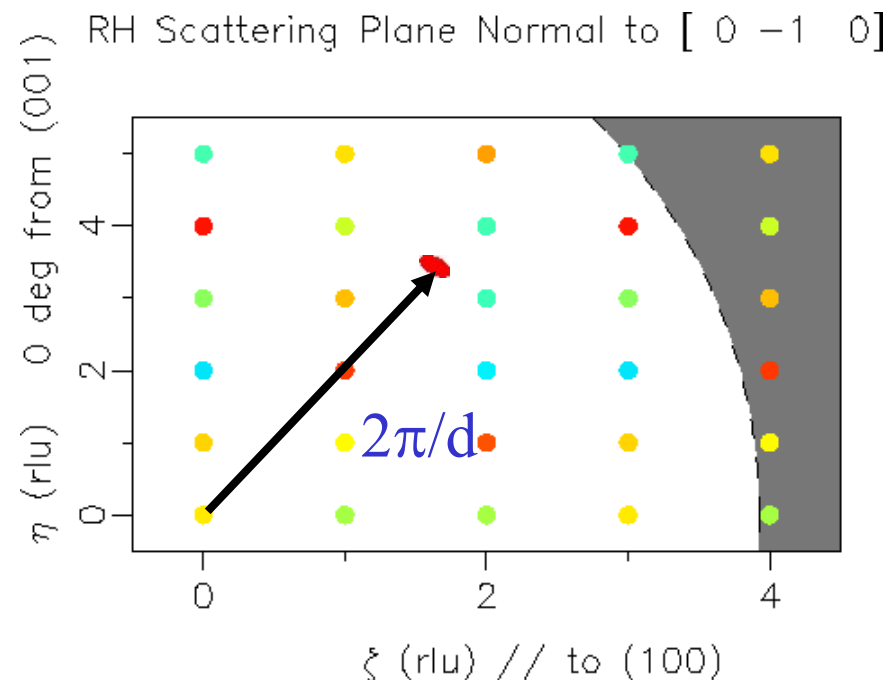
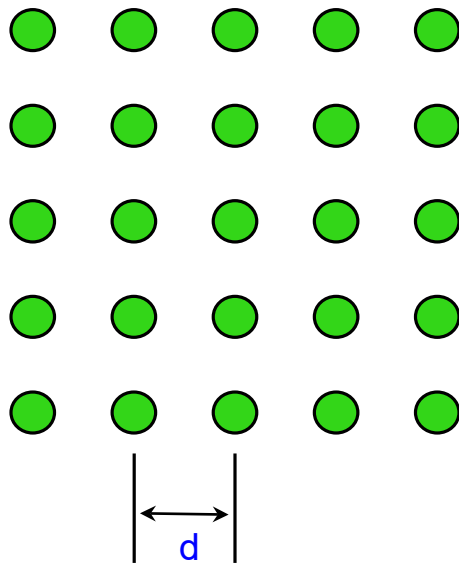
$$\Phi = F\{\vec{r}_i(t), \vec{r}_j(t), \vec{S}_i(t), \vec{S}_j(t)\}$$



Φ provides information about all of these quantities!

Reciprocal (Scattering) Space

Periodic array of atoms in Real Space



Real space \leftrightarrow Reciprocal (Fourier) Space

NCNR

Other Probes



$$E_{neutron}(\text{meV}) = 2.0719k^2 = 81.7968 / \lambda^2$$

$$E_{photon}(\text{keV}) = 2.0k = 12.4 / \lambda$$

$$E_{electron}(\text{eV}) = 3.8k^2 = 150 / \lambda^2$$

$\lambda = 1 \text{ \AA}$: $E_n = 82 \text{ meV}$; $E_p = 12,400,000 \text{ meV}$; $E_e = 150,000 \text{ meV}$

$$1 \text{ meV} = 11.6 K \quad (k_B T) \qquad \qquad 300 \text{ K} \rightarrow 25 \text{ meV}$$

$$1 \text{ meV} = 8.06 \text{ cm}^{-1} \quad (E / hc)$$

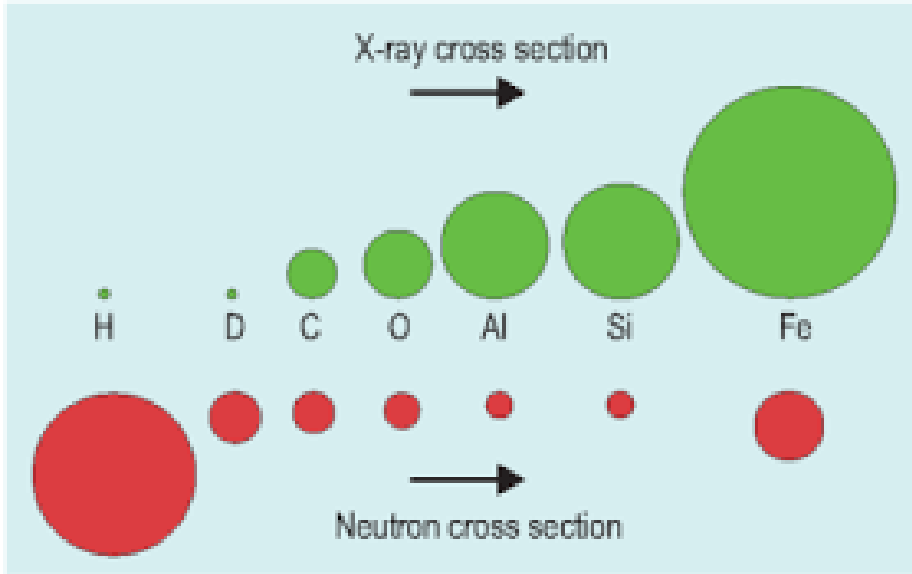
$$1 \text{ meV} = 0.2418 \text{ THz} \quad (E / h)$$

$$1 \text{ meV} / \mu_B = 17.3 T \quad (E / \mu_B)$$

Neutron and X-ray Scattering

- Both techniques collect data as functions of the energy and the momentum transferred from the system to the neutron or photon beam. The resulting five-dimensional data sets serve as powerful probes of materials. Elastic scattering elucidates the crystal structure, magnetic configuration, direction of the spins, symmetry of the magnetic state, spatial distribution of the magnetization density, and dependence of the order(s) parameter on thermodynamic fields such as temperature, pressure, magnetic and electric fields. Inelastic scattering determines the energies of the fundamental excitations which can be used to elucidate the nature, strength, and range of the interactions.
- Both techniques can measure crystal and magnetic structures and their dynamics.
- Neutron advantages:
 - Magnetic and structural scattering are comparable in strength; Elastic scattering yields quantitative information; energy resolution is orders-of-magnitude better than x-rays; simplicity of sample environment; low T accessible. Theory has solid theoretical basis.
- X-ray advantages:
 - High Flux → small samples; individual domains, topography; pump probe capability; resonant x-ray scattering → element specific; magnetic resonant x-ray scattering; RIXS

Neutrons and X-rays are Complementary



Nucleus looks like a point particle → b is just a constant independent of scattering angle.

Adjacent elements, heavy + light elements, isotope substitution

Neutron Cross Sections

$$I_N(\mathbf{g}) = CM_\tau A(\theta_B) |F_N(\mathbf{g})|^2$$

$$|F_N(\mathbf{g})|^2 = \left| \sum_j b_j e^{i\mathbf{g} \cdot \mathbf{r}_j} e^{-W_j} \right|^2$$

$$I_M(\mathbf{g}_{hkl}) = C \left(\frac{\gamma e^2}{2mc^2} \right)^2 M_g A(\theta_B) |F_M(\mathbf{g}_{hkl})|^2$$

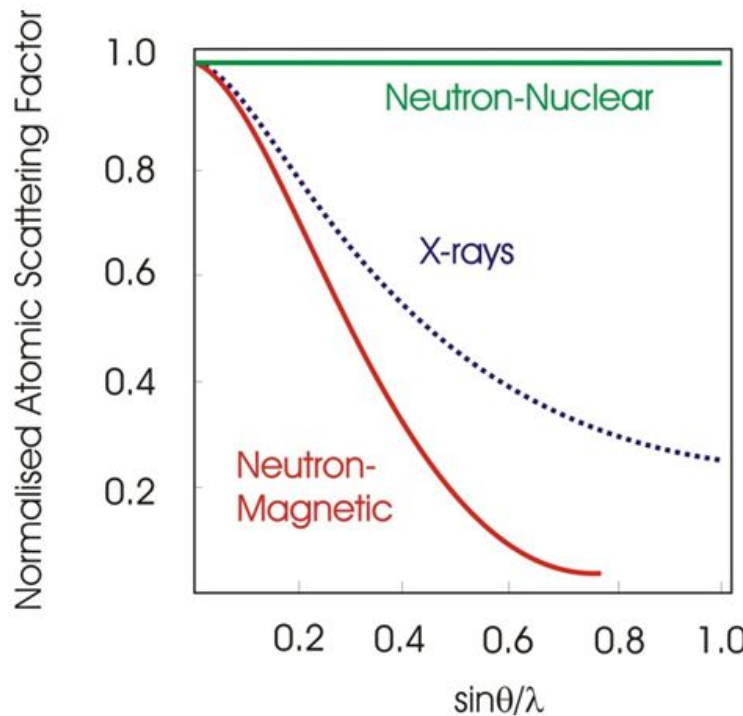
$$F_M(\mathbf{g}_{hkl}) = \sum_{j=1}^N e^{ig \cdot \mathbf{r}_j} \hat{\mathbf{g}} \times \left[\mathbf{M}_j(\mathbf{g}) \times \hat{\mathbf{g}} \right] e^{-W_j}$$

$$|F_M(\mathbf{g})|^2 = \left\langle 1 - \left(\hat{\mathbf{g}} \cdot \hat{\boldsymbol{\eta}} \right)^2 \right\rangle \left\langle \hat{\boldsymbol{\mu}}^z \right\rangle^2 f^2(\mathbf{g}) \left| \sum_j \eta_j e^{i\mathbf{g} \cdot \mathbf{r}_j} e^{-W_j} \right|^2$$

Neutrons and X-rays are Complementary

magnetic scattering amplitude for an ion is related to the Fourier Transform of the total magnetisation density, $M(r)$::

$$M(q) = \int M(r) \exp[i(q \cdot r)] d^3r$$



As the magnetism arises from unpaired electrons in *outer shells* and not the nucleus there is a dependence on intensity, similar to the $\sin(\theta)/\lambda$ used for x-rays

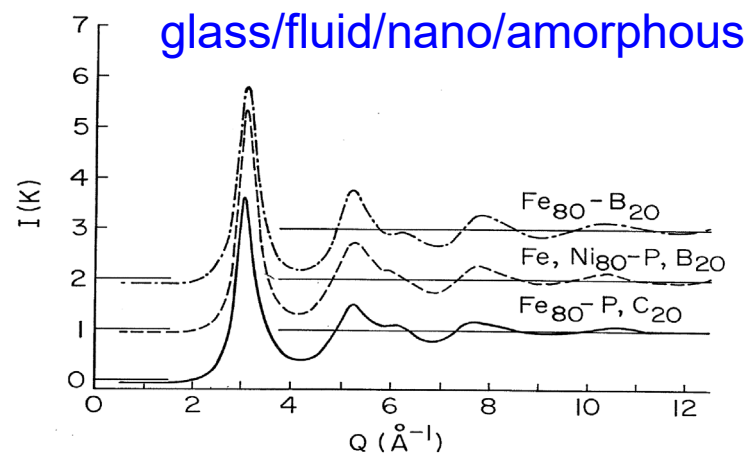
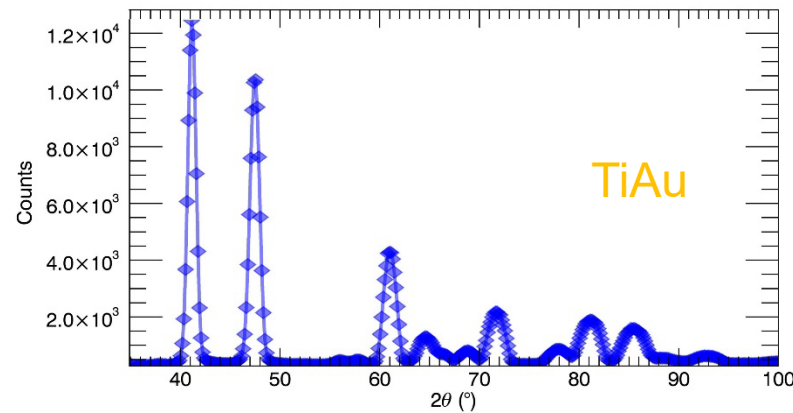
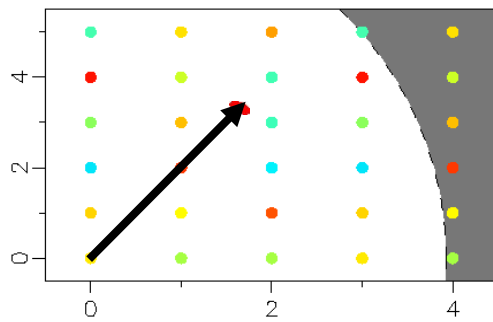
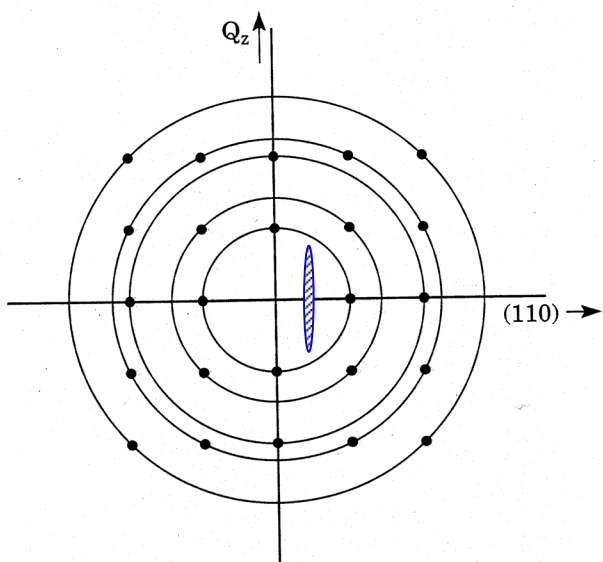
Magnetic X-ray Cross Sections

$$F_j(E) = \sigma^{(0)}(E) \varepsilon_i \cdot \varepsilon_o^* + \sigma^{(1)}(E) \varepsilon_i \times \varepsilon_o^* \cdot M_j + \sigma^{(2)}(E) \left((\varepsilon_i \cdot M_j)(\varepsilon_o^* \cdot M_j) - \frac{1}{3} \varepsilon_i \cdot \varepsilon_o^* \right)$$

$$I = \left| \sum_j e^{ig \cdot r_j} \sigma_j^{(1)}(E) \varepsilon_i \times \varepsilon_o^* \cdot M_j \right|^2$$

Reciprocal Space for Powder

NCNR

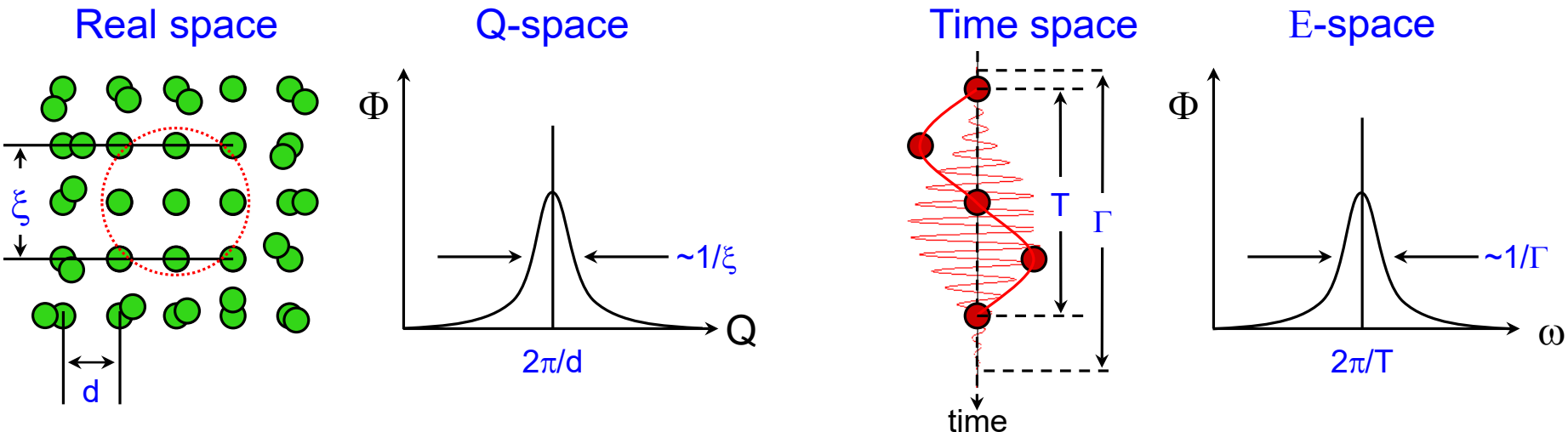


Correlations

NCNR

The scattered neutron flux $\Phi(Q, \hbar\omega)$ is proportional to the space (r) and time (t) Fourier transform of the probability $G(\vec{r}, t)$ of finding one or two atoms (**spins**) separated by a particular distance (**angle**) at a particular time.

$$\Phi \propto \frac{\partial^2 \sigma}{\partial \Omega \partial \omega} \propto \iint e^{i(\vec{Q} \cdot \vec{r} - \omega t)} G(\vec{r}, t) d^3 \vec{r} dt$$



Neutron Scattering Techniques

Diffraction

- **Crystallography**—powder, single crystal
Atomic positions, site occupancies, lattice parameters, bond distances, mean-square vibrations as a function of T, H, P, E, ...
- **Magnetism**
Magnetic structure, order parameter, spin directions, spin density distribution
Phase Transitions and Critical Phenomena (Scaling, Universality)
- **Small Angle Neutron Scattering (SANS)**
Ferromagnetic Correlations, Vortex Structures, Domain Structures, Grain boundaries, twin boundaries, defect structures, nanoparticles, skyrmions, ...
- **Thin Film Reflectometry**
Density profiles, Magnetic structures, Magnetization profiles, Surface and Interface properties (flatness, roughness)

Inelastic Scattering

Lattice Dynamics

Phonon Dispersion, Density of States

Interatomic Force constants

Mean-square vibrations

Diffusion

Spin Dynamics

Magnon Dispersion, Exchange interactions

Magnetic Anisotropy

Magnetic Fluctuation Behavior

Crystal Field Levels

Magnetic-Structural Coupling

NIST Center for Neutron Research



May 2017

Oak Ridge National Laboratory



High Flux Isotope
Reactor

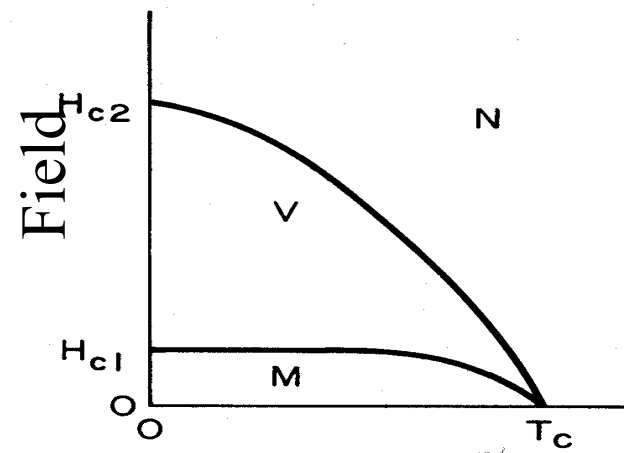
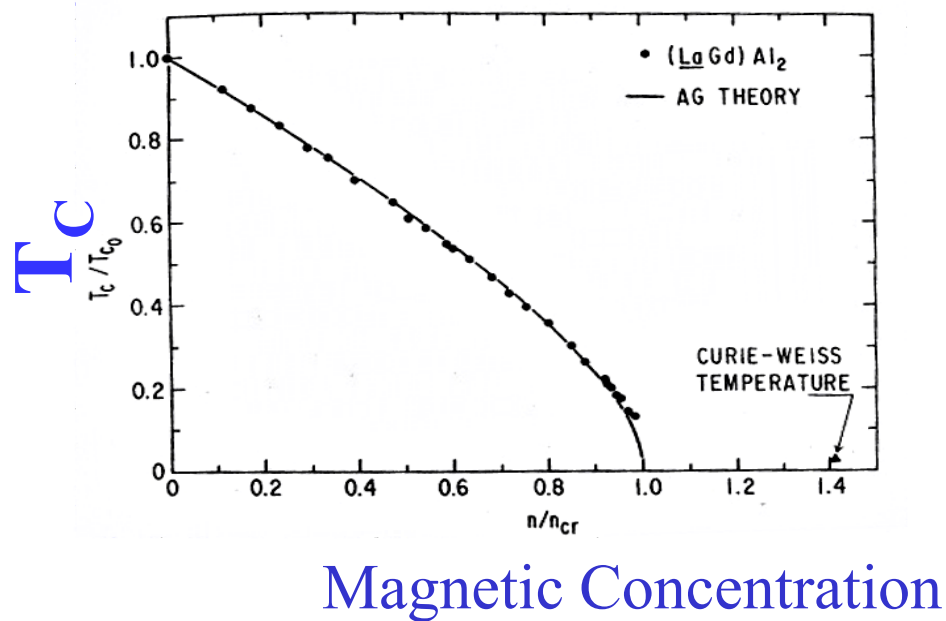


Spallation Neutron
Source

Materials that are both Magnetic and Superconducting

Magnetic Impurities
Cause Spin depairing

Magnetic Fields and
Superconductivity are Antagonists



M. B. Maple, Appl. Phys. 9, 179 (1976)

Magnetic Superconductor History

- Pure Superconductors (1911→...)
- **X** Magnetic Impurities **X**
- Concentrated Magnetic Systems (Exceptions to the Rule!)
 C-15 Cubic Laves phase ($\text{Ce-Ho}\text{Ru}_2$) ('60's-'70's)
- Magnetic Sublattice—Long Range Order
 Chevrel Phase DyMo_6S_8 ('70's)
- Ferromagnets—Competition & Coexistence
 - Chevrel Phase $\text{HoMo}_6(\text{S-Se})_8$, ErRh_4B_4 ('70's – 80's)
- High T_C cuprates—Cu spin order & fluctuations
 Cuprates $\text{RBa}_2\text{Cu}_3\text{O}_7$ [123], R_2CuO_4 [214] ('80's→...)
- Borocarbides
 - $\text{HoNi}_2\text{B}_2\text{C}$, $\text{ErNi}_2\text{B}_2\text{C}$ ('90's→...)
- New Ferromagnetic Superconductors
 - Ruthenates $\text{RuSr}_2\text{GdCu}_2\text{O}_8$, $\text{RuSr}_2(\text{Eu-Ce})_2\text{Cu}_2\text{O}_{10}$; ZrZn_2 , UGe_2 (2000's→...)
- Sodium cobaltates (Magnetic, thermoelectric, and Superconducting) 2000's→...
 - Na_xCoO_2 (+ H₂O) [just add water for superconductivity !]
- Iron-based superconductors (2008→...)
 - $\text{R}(\text{O}_{1-x}\text{F}_x)\text{FeAs}$; $\text{Sr}_{1-x}\text{K}_x\text{Fe}_2\text{As}_2$; LiFeAs ; $\text{Fe}(\text{Se}_{1-x}\text{Te}_x)$
 - 1:1:1:1 1:2:2 1:1:1 1:1



Ferromagnetic Superconductors

(Ce-Ho)Ru₂

HoMo₆S₈, HoMo₆Se₈, ErRh₄B₄

ErNi₂B₂C

RuSr₂GdCu₂O₈ & RuSr₂Eu_{2-x}Ce_xCu₂O₁₀

(Li-Fe)OHFeSe

UGe₂ ZrZn₂, UCoGe, URhGe, C/S

Magnetic Structures

Ferromagnet



Antiferromagnet

Spin Density Wave

Magnetic Structures

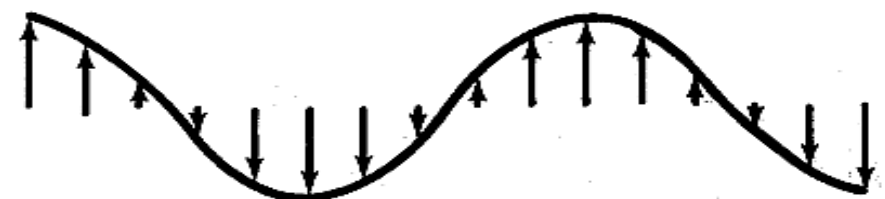
Ferromagnet



Antiferromagnet



Spin Density Wave



Chevrel Phase Superconductors

HoMo_6S_8 , HoMo_6Se_8 , ErRh_4B_4

$[(\text{HoS}_8)\text{Mo}_6]$ Magnetic Lattice Isolated]

$T_{\text{super}} = 1.8 \text{ K}$

5.6 K

8.6 K

$T_{\text{ferro}} = 0.7 \text{ K}$

0.5 K

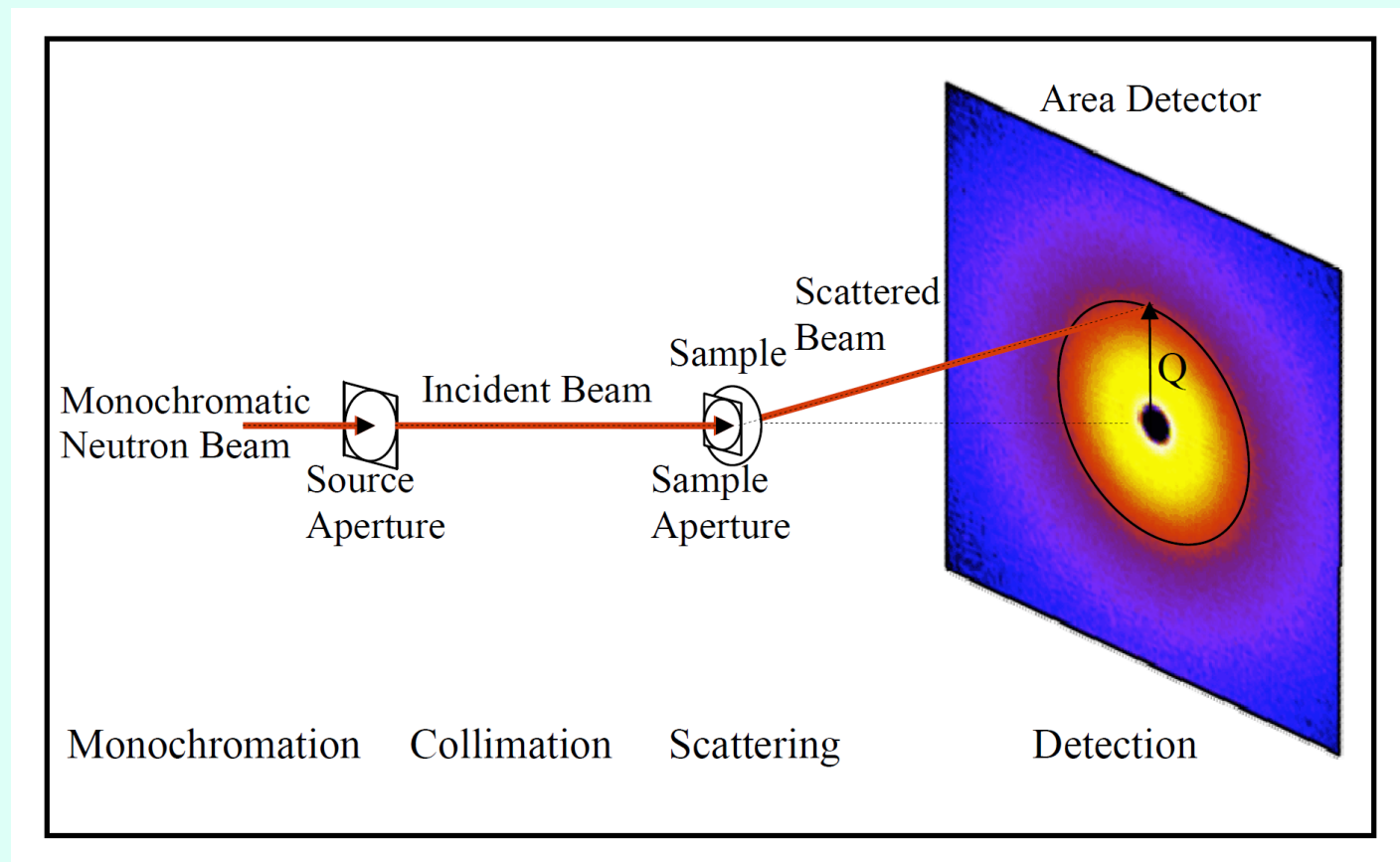
0.9 K

$T_{\text{reentrant}} = 0.7 \text{ K}$

$< 0 \text{ K}$

0.9 K

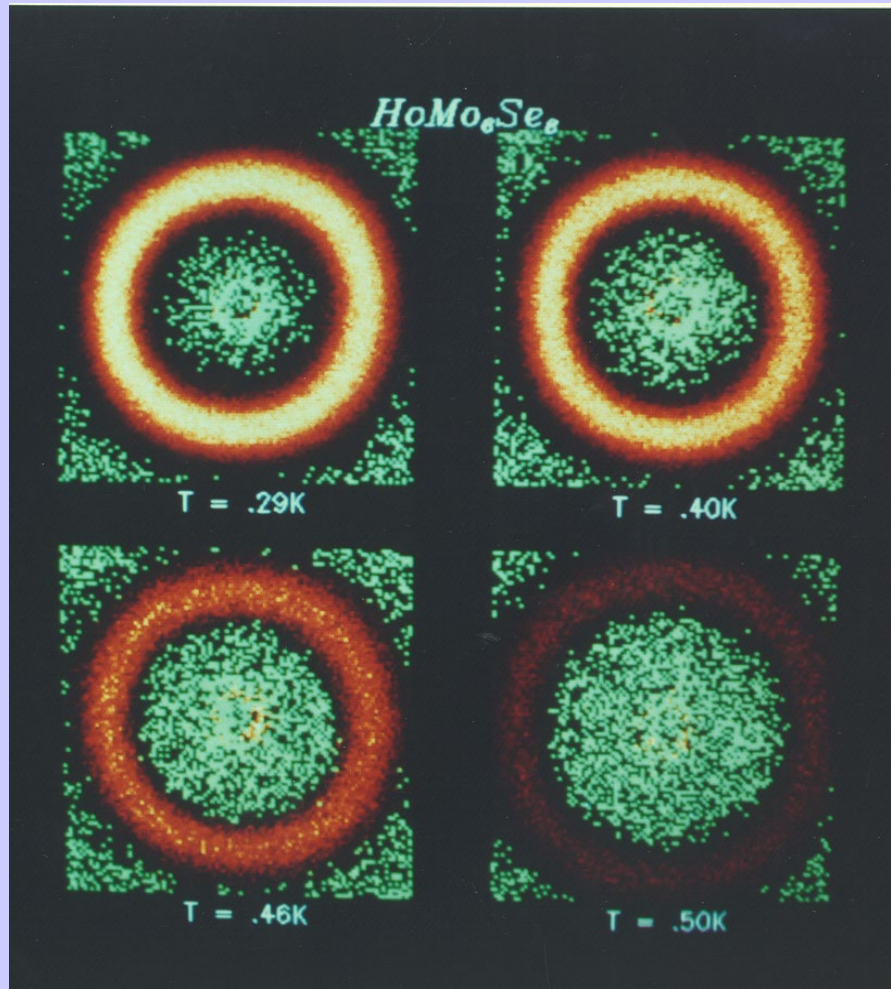
Small Angle Neutron Scattering



HoMo_6Se_8

$T_S = 5.6 \text{ K}$

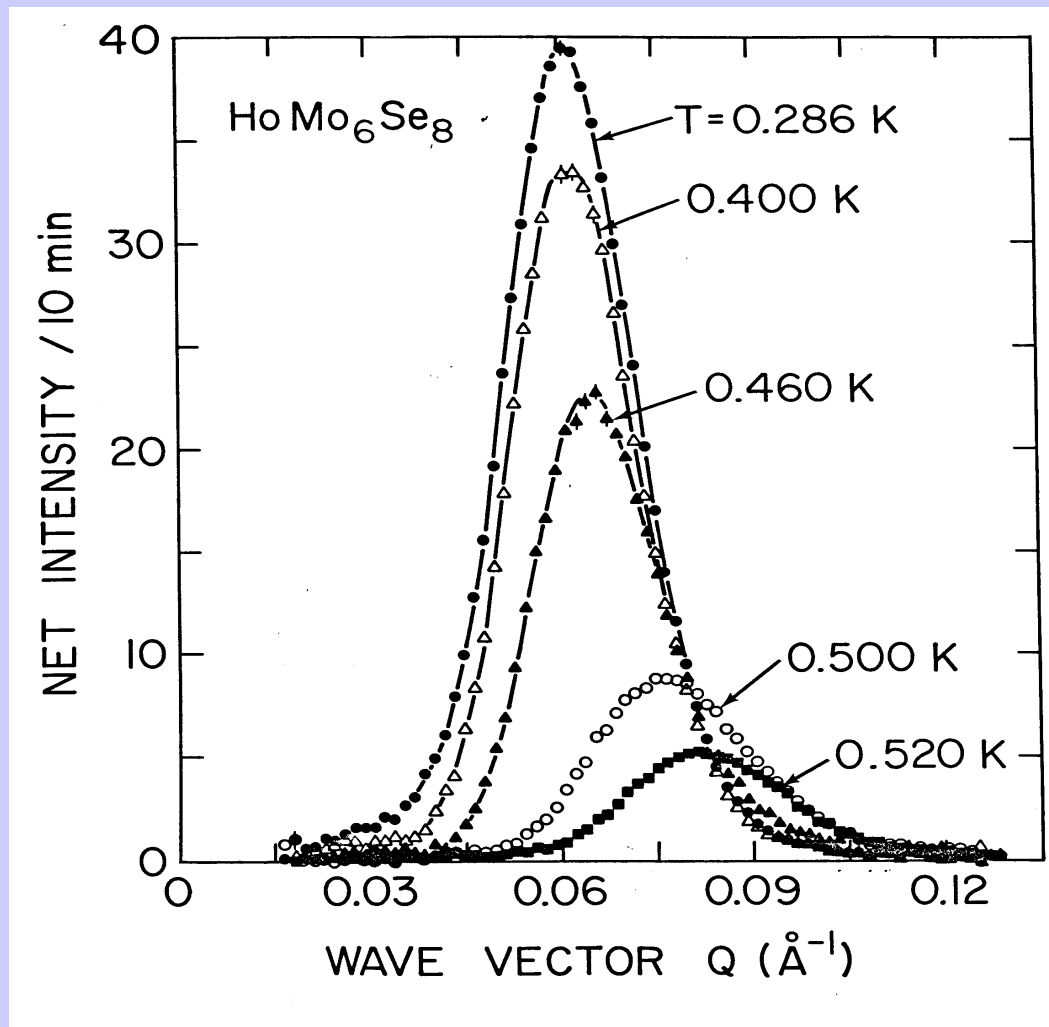
$T_M = 0.5 \text{ K}$



$\sim 100 \text{ \AA}$
(10 nm)
periodicity

J. W. Lynn, J. A. Gotaas, R. W. Erwin, R. A. Ferrell, J. K. Bhattacharjee, R. N. Shelton and P. Klavins,
Phys. Rev. Lett. **52**, 133 (1984)

HoMo_6Se_8



NIST Center for Neutron Research

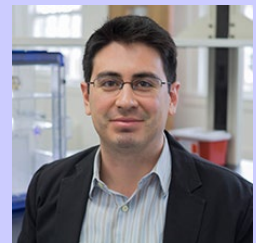
NCNR

Iron-based High T_c Superconductors

Iron-based superconductors under Investigation at the NCNR

- FeSe, $\text{Fe}_{1+x}(\text{Se}-\text{Te})$, $\text{K}_x\text{Fe}_{2-y}\text{Se}_2$ (1:1)
- LiFeAs (1:1:1)
- $\text{LaO}_{1-x}\text{F}_x\text{FeAs}$ LaOFeAs (1:1:1:1)
- $\text{CeO}_{1-x}\text{F}_x\text{Fe}(\text{As},\text{P})$ CeOFeAs
- $\text{NdO}_{1-x}\text{F}_x\text{FeAs}$ Nd...
- $\text{PrO}_{1-x}\text{F}_x\text{FeAs}$ Pr...
- BaFe_2As_2 , SrFe_2As_2 , CaFe_2As_2 (1:2:2)
- CaFe_2As_2 , Under Pressure; doping
 - <https://www.nist.gov/people/jeffrey-w-lynn>

${}^7\text{Li}_{1-x}\text{Fe}_x\text{ODFeSe}$



Neutron Investigation of the Magnetic Scattering in an Iron-based Ferromagnetic Superconductor

Jeffrey W. Lynn¹, Xiuquan Zhou², Christopher K. H. Borg², Shanta R. Saha³, Johnpierre Paglione³, and Efrain E. Rodriguez²

Phys. Rev. B **92**, 060510(R) (2015).

*The Preparation and Phase Diagram of Superconducting
 $({}^7\text{Li}_{1-x}\text{Fe}_x\text{OD})\text{FeSe}$*

Xiuquan Zhou², Christopher K. H. Borg², Jeffrey W. Lynn¹, Shanta R. Saha³, Johnpierre Paglione³, and Efrain E. Rodriguez²,
J. Mater. Chem. C **4**, 3934 (2016).

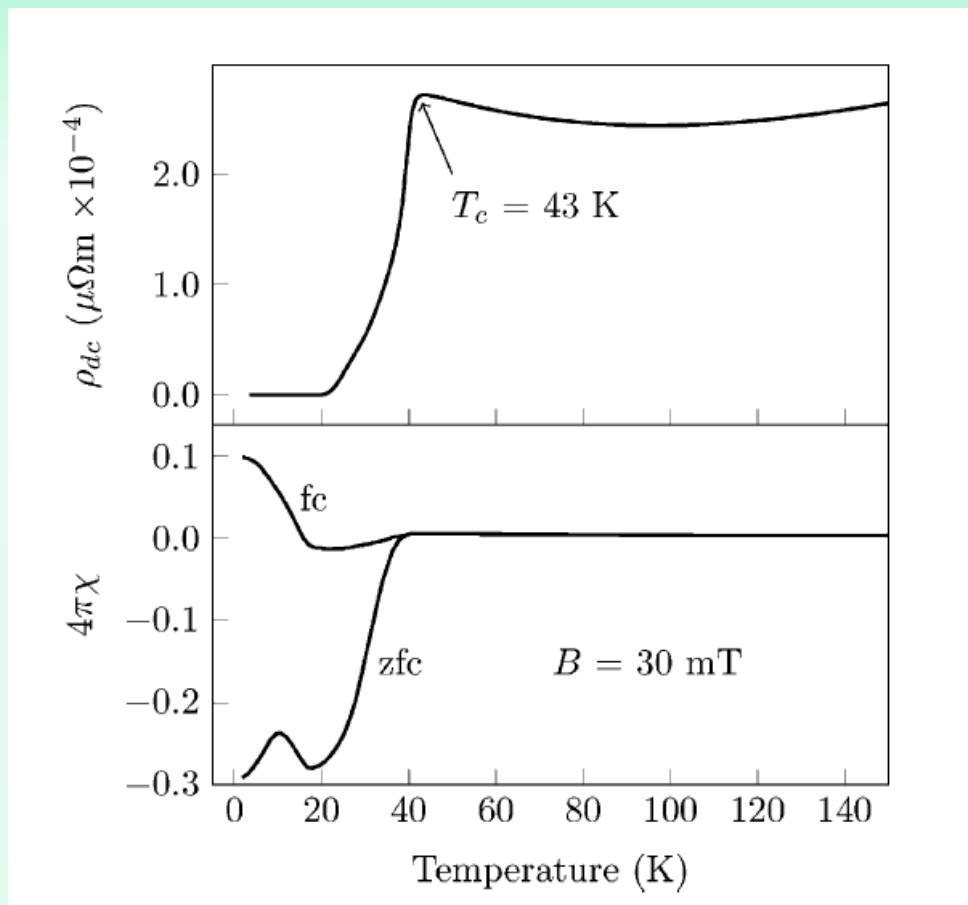
Long range magnetic order in Mn-doped $(\text{LiOH})\text{FeSe}$, Brandon Wilfong, Xiuquan Zhou, Huafei Zhang, Navneeth Babra, Craig M. Brown, Jeffery W. Lynn, Simon A. J. Kimber, Keith M. Taddei, Johnpierre Paglione, and Efrain E. Rodriguez, Phys. Rev. Materials **4**, 034803 (2020).

¹NIST Center for Neutron Research, Gaithersburg, MD (USA)

²Department of Chemistry and Biochemistry, University of Maryland, College Park, MD (USA)

³Department of Physics, University of Maryland, College Park, MD (USA)

(Li-Fe)OHFeSe Ferromagnetic Superconductor

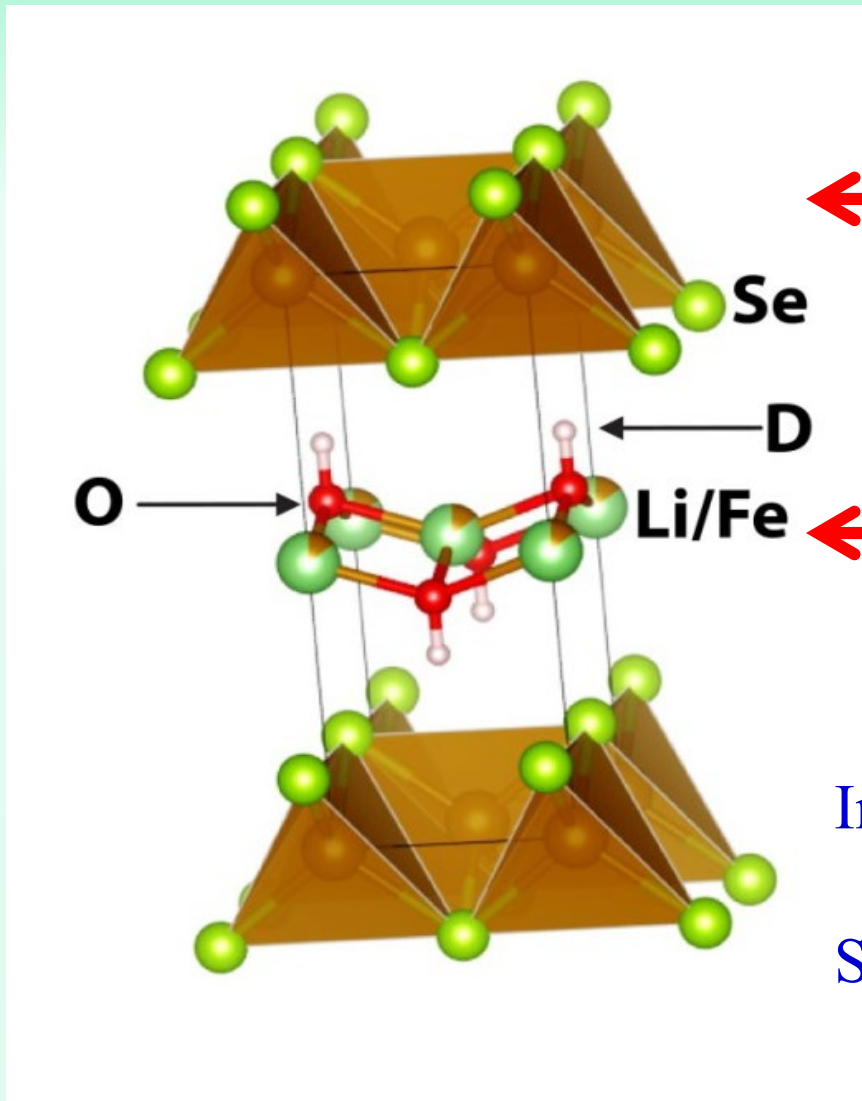


$T_S = 43$ K

$T_F = 10$ K

Coexistence of 3d-ferromagnetism and superconductivity in $[(\text{Li}_{1-x}\text{Fe}_x)\text{OH}](\text{Fe}_{1-y}\text{Li}_y)\text{Se}$, Ursula Pachmayr, Fabian Nitsche, Hubertus Luetkens, Sirko Kamusella, Felix Bruckner, Rajib Sarkar, Hans-Hennig Klauss, and Dirk Johrendt, Angew. Chem. Int. Ed. **54**, 293 (2015)

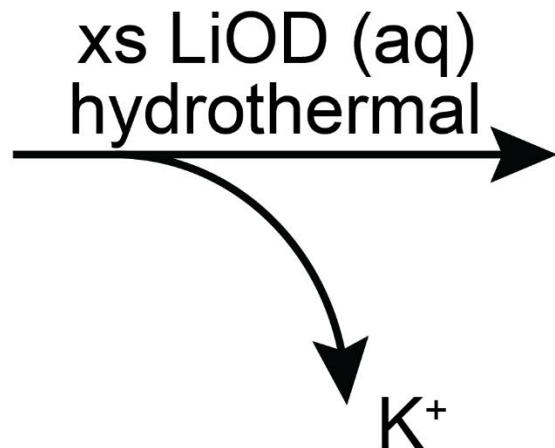
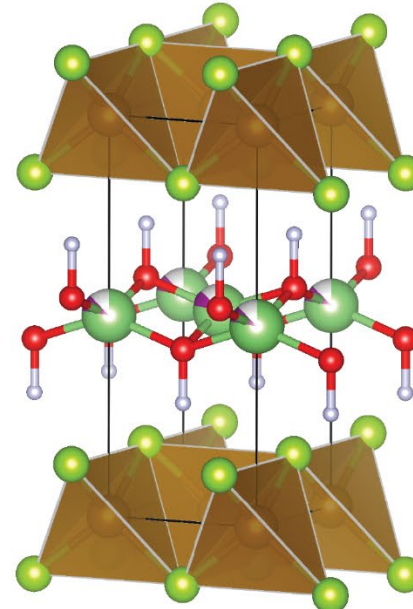
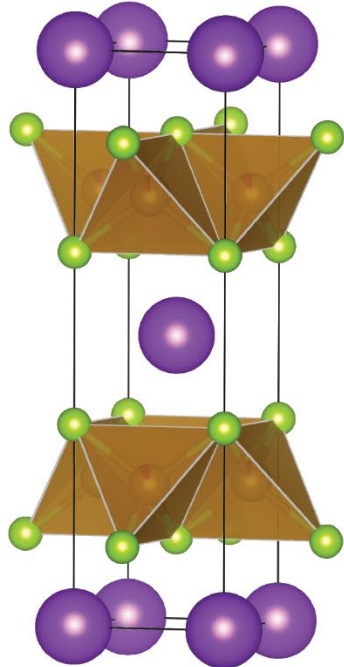
Crystal Structure



← FeSe Superconducting Layer
Se
D
O ← Magnetic Layer
Li/Fe

Incommensurate Long wavelength
Ordered state?
Spontaneous Vortex Lattice?

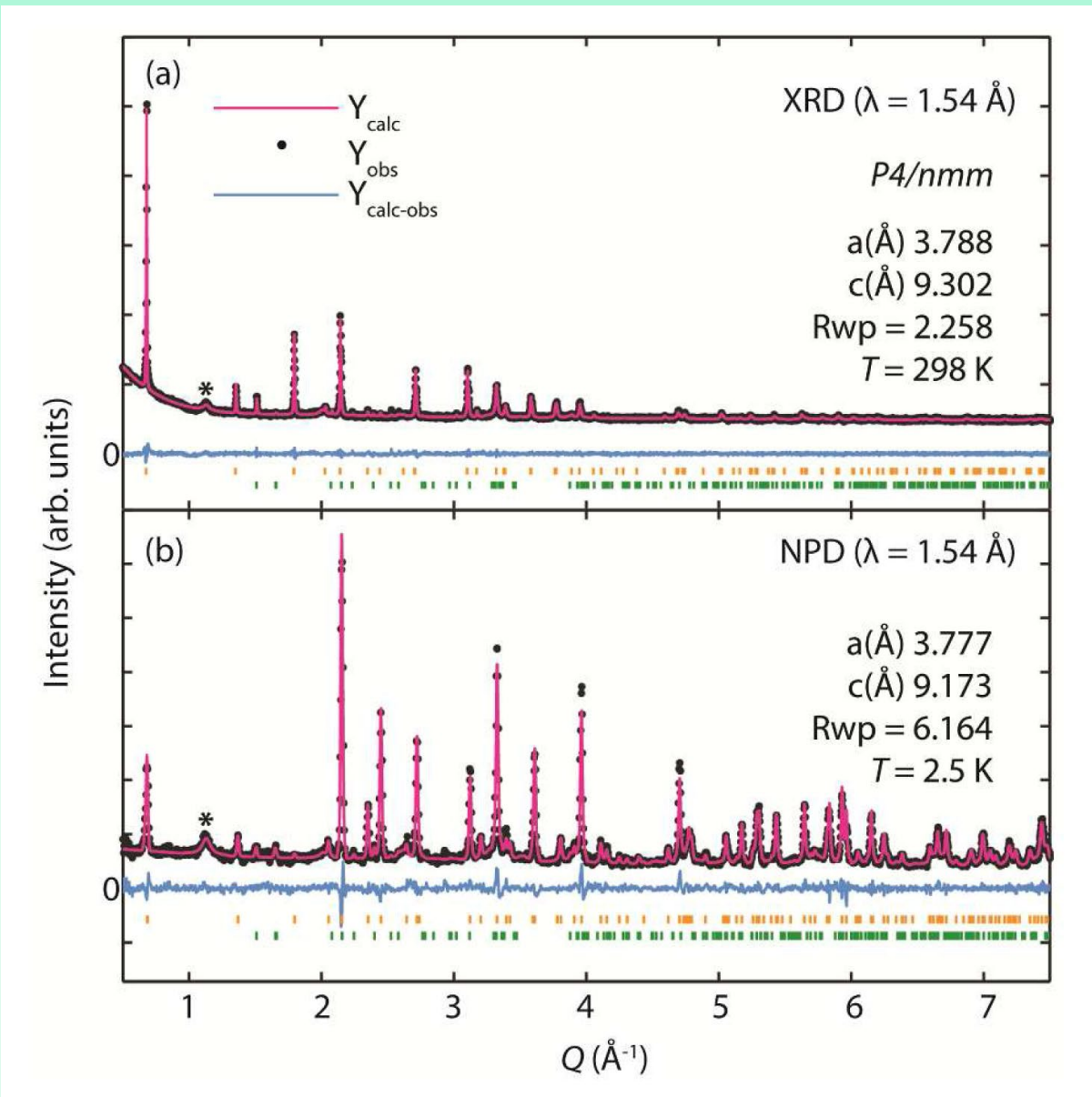
Synthesis and Structure



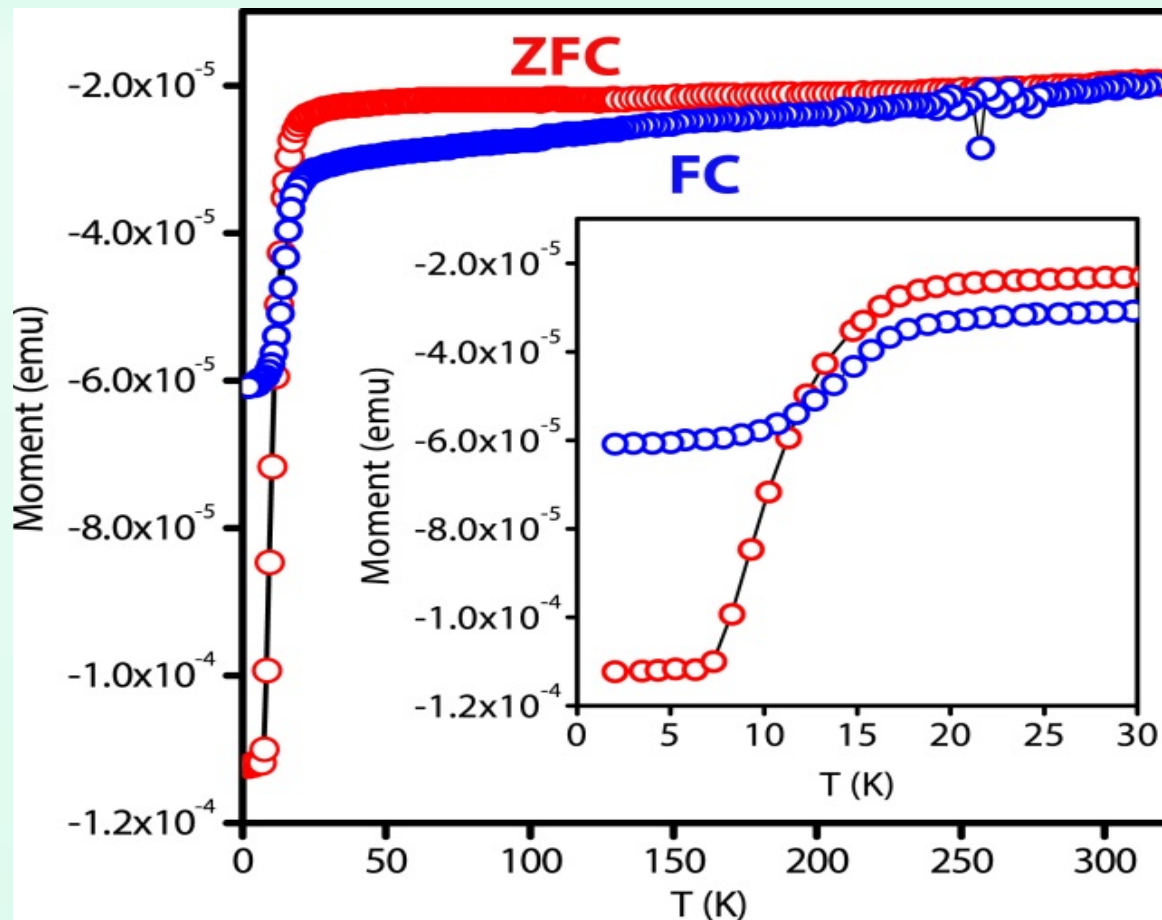
$\text{K} + \text{Fe} + \text{Mn} + \text{Se}$
self-flux method



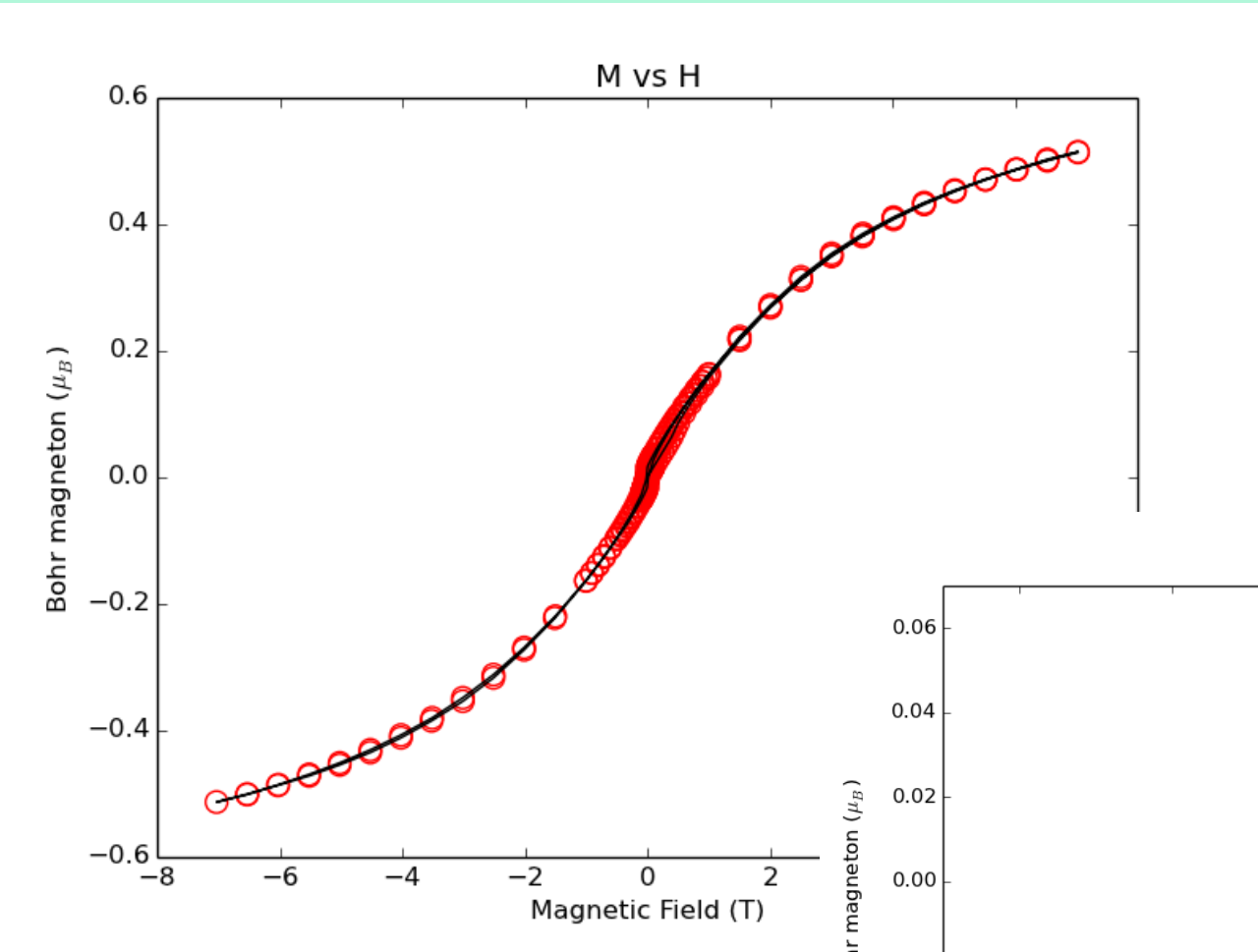
Neutron and X-ray Diffraction



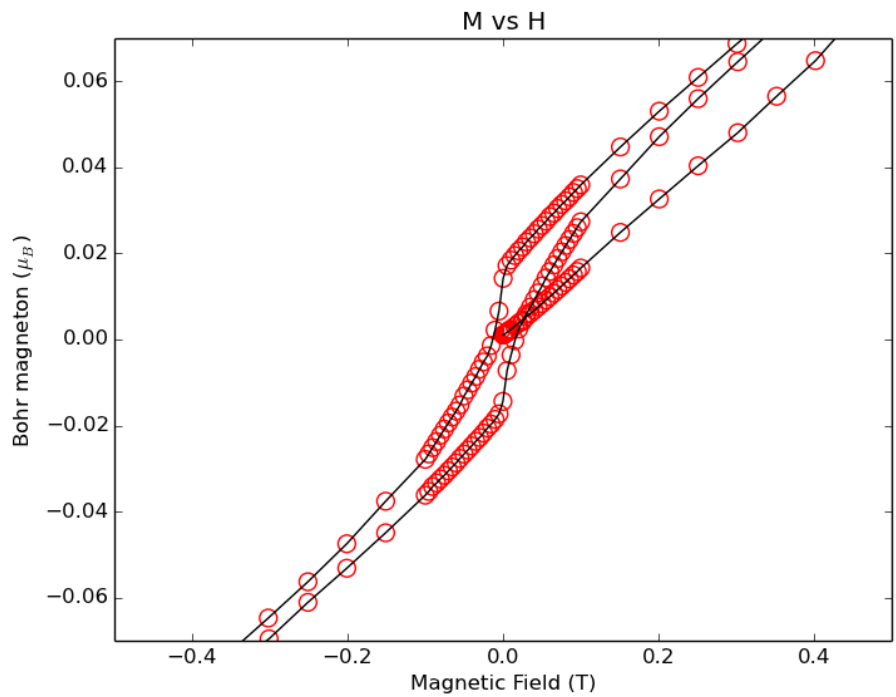
Magnetization for $T_c = 18$ K (polycrystalline sample)



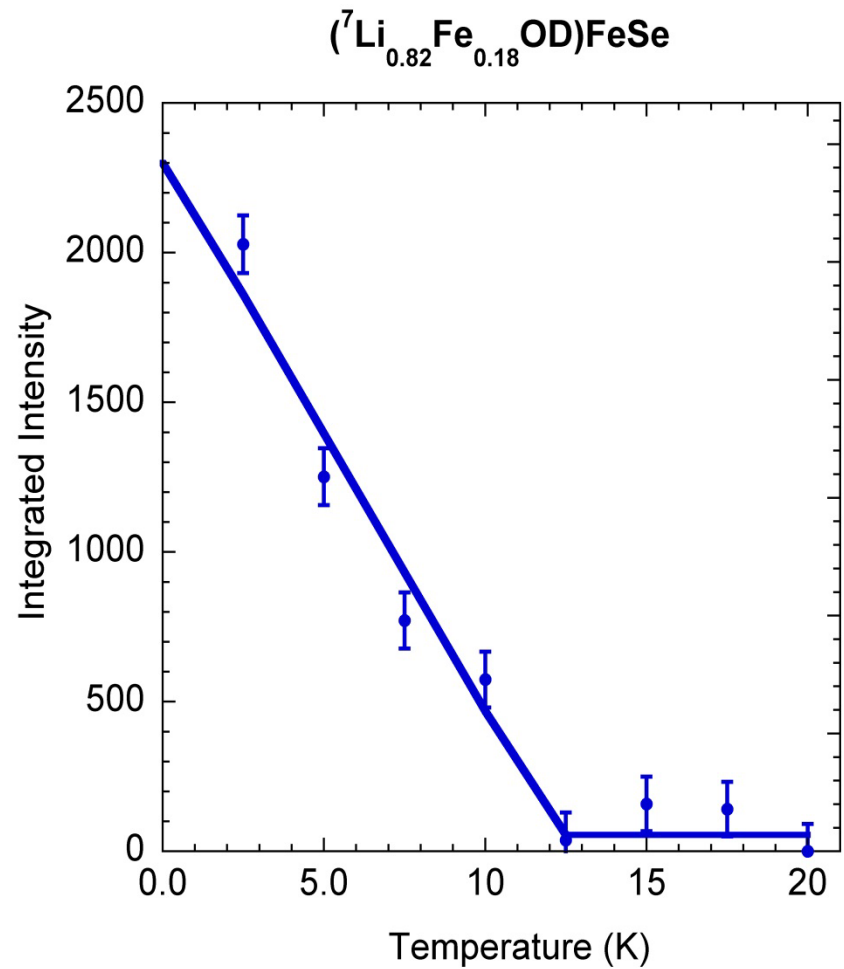
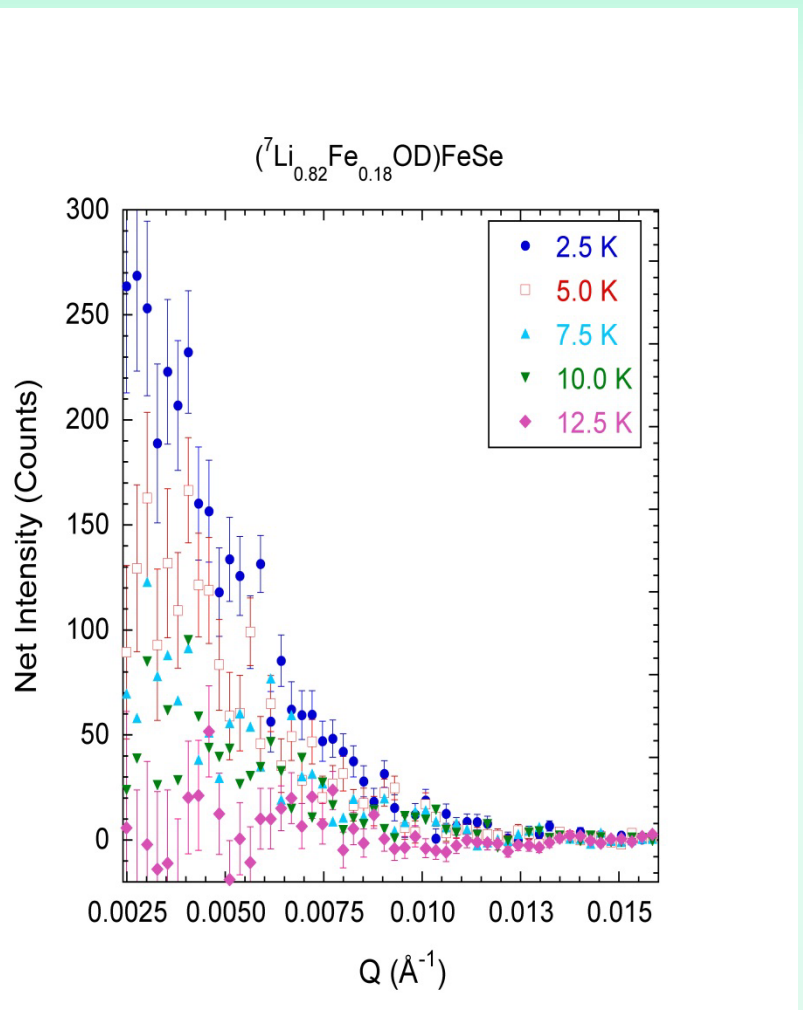
Ferromagnetic Magnetization



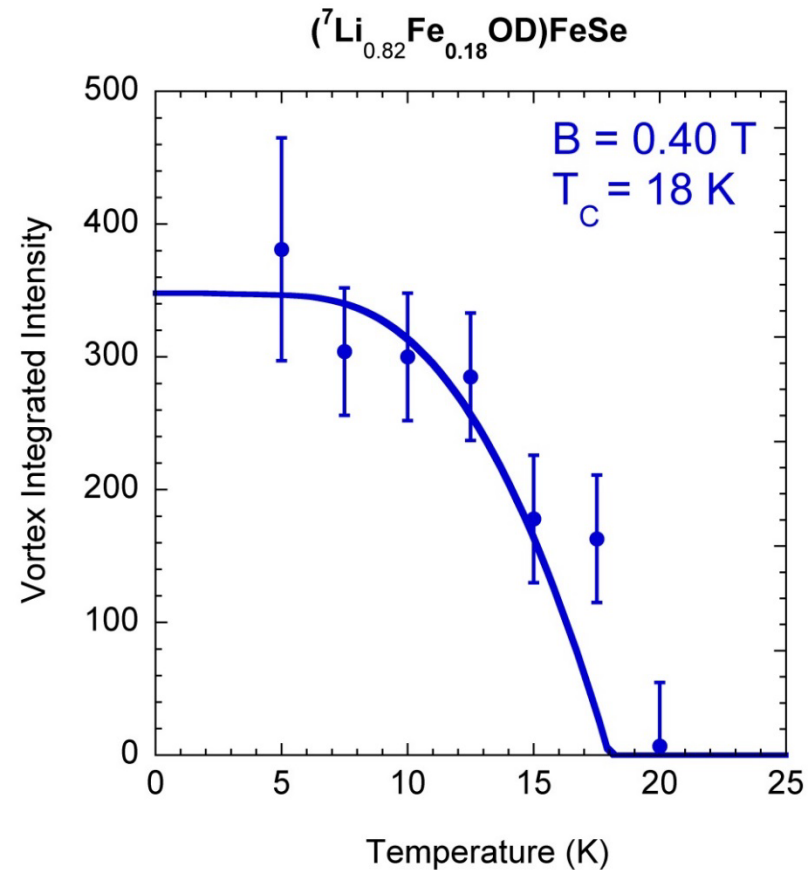
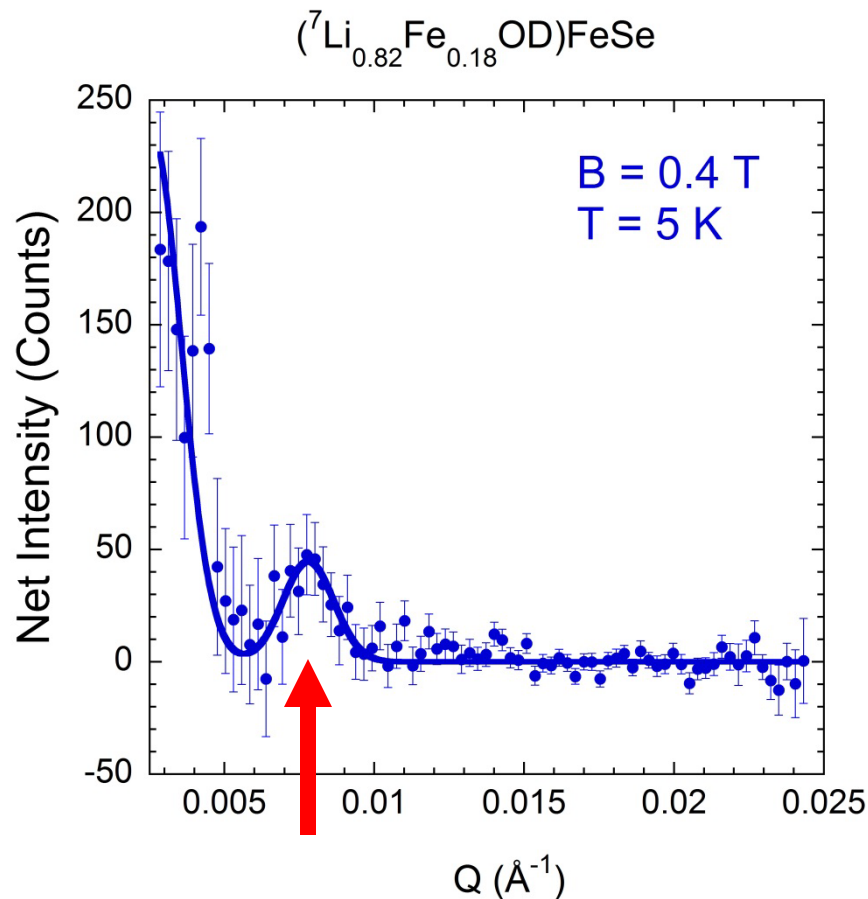
2 K



No Applied Magnetic Field

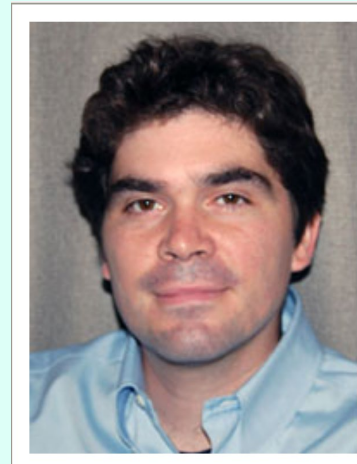
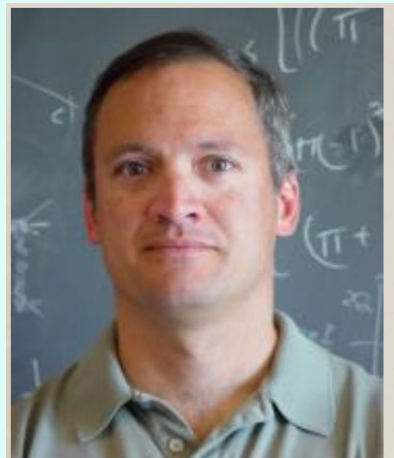
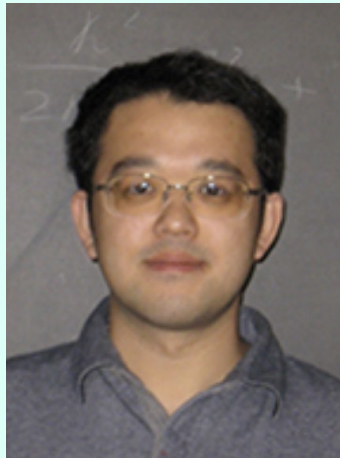


B = 0.4 T



Singular angular magnetoresistance in a magnetic nodal semimetal

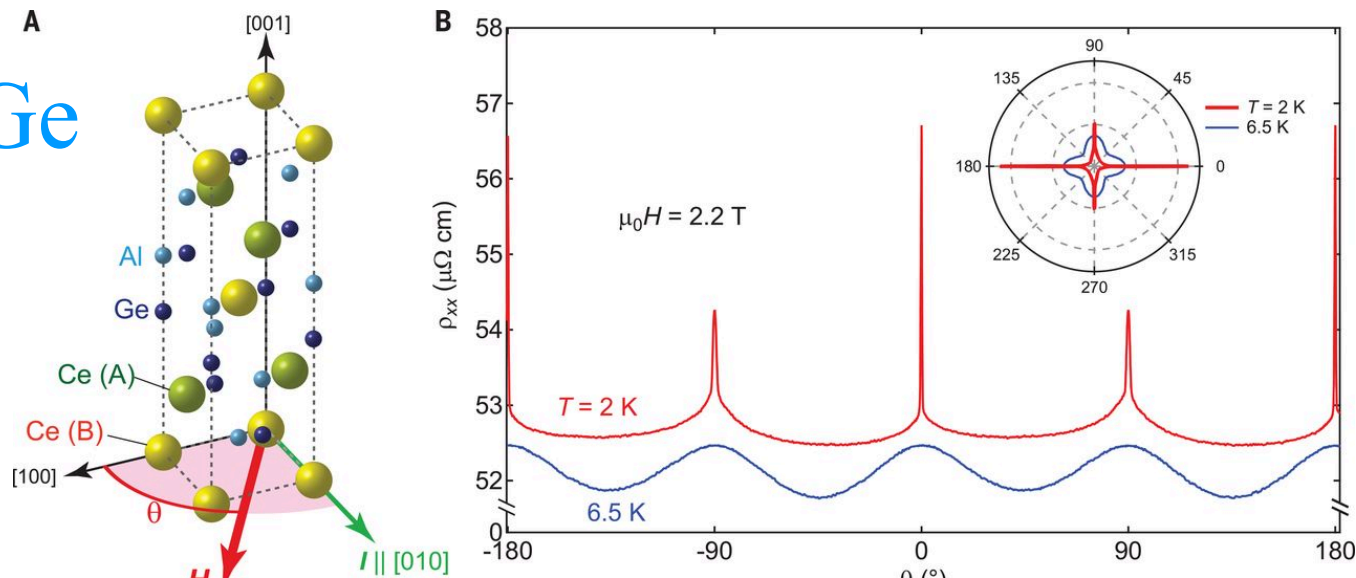
by *T. Suzuki, L. Savary, J.-P. Liu, J. W. Lynn, L. Balents, and J. G. Checkelsky*



Science
Volume 365(6451):377-381
July 26, 2019

Fig. 1 Singular angular magnetoresistance (SAMR).

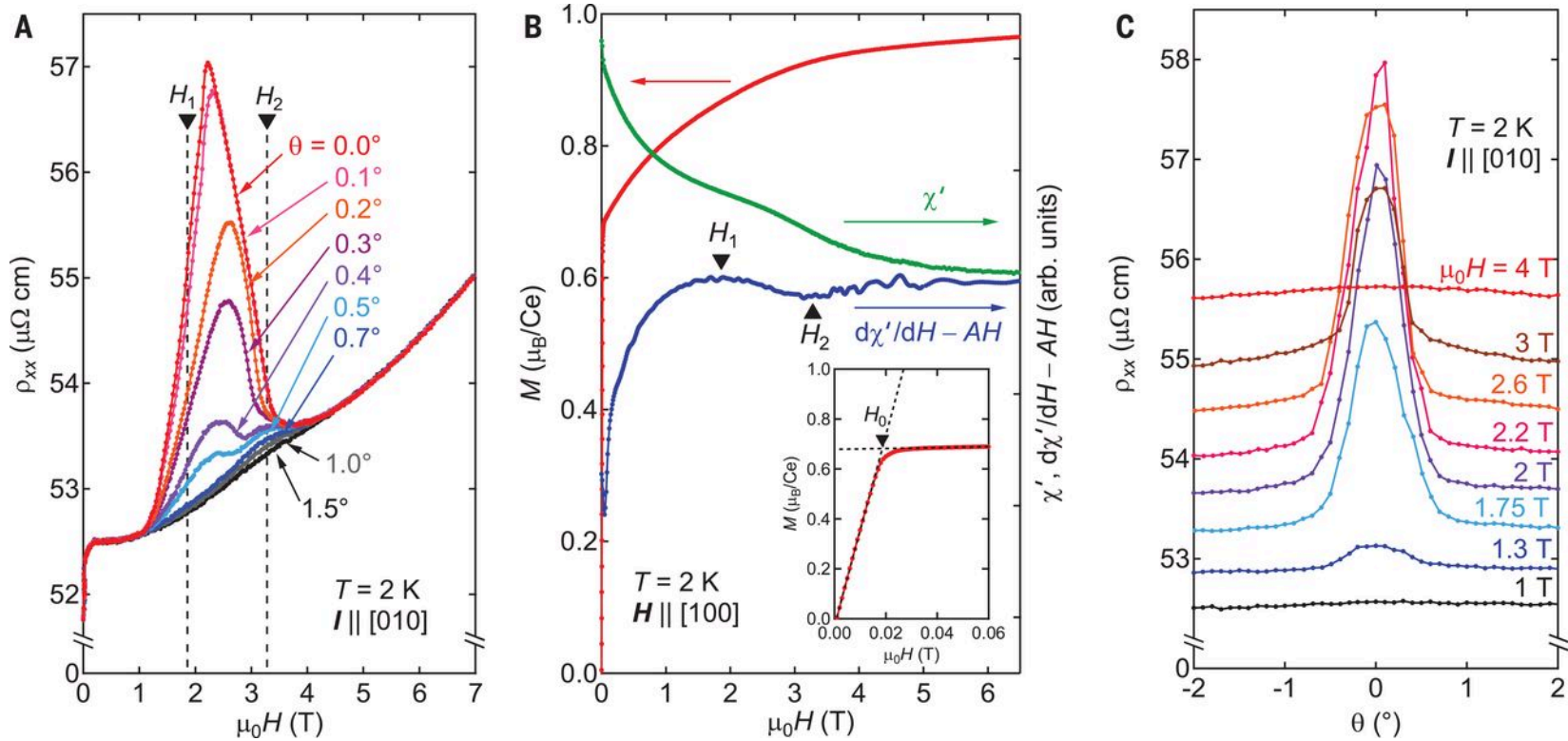
CeAlGe



T. Suzuki et al. Science 2019;365:377-381

Science
AAAS

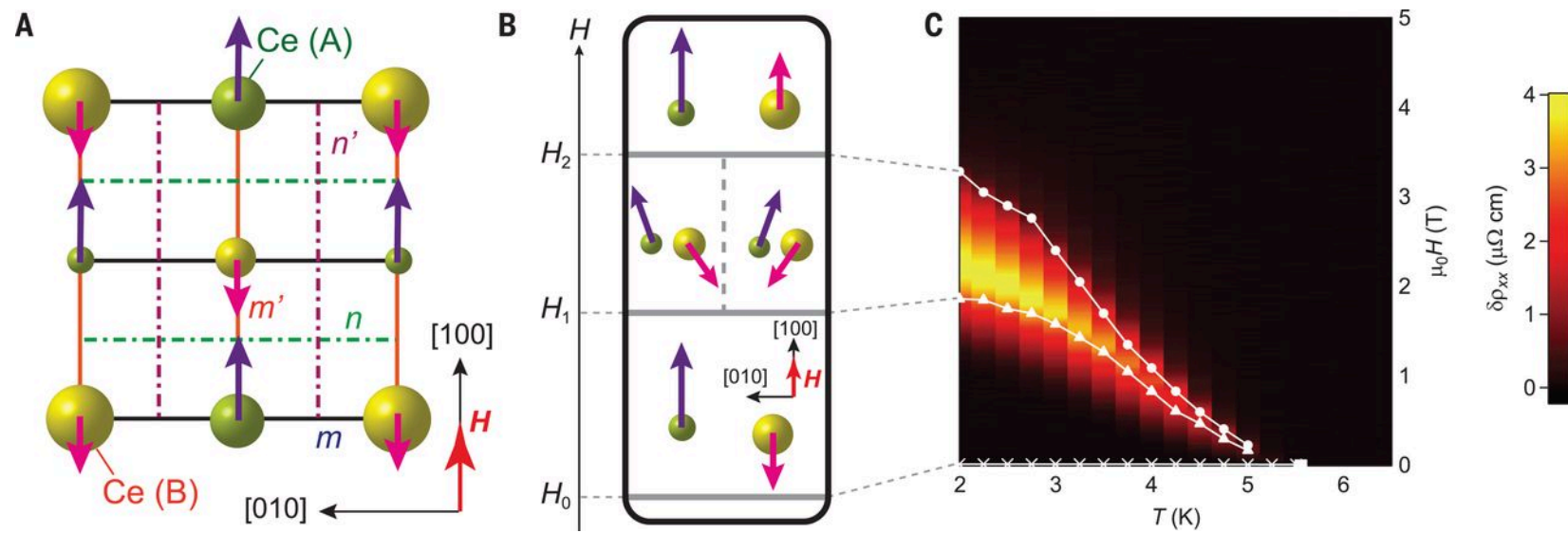
Fig. 2 Magnetic field dependence of SAMR.



T. Suzuki et al. Science 2019;365:377-381

Science
AAAS

Fig. 3 Phase diagram of SAMR.



T. Suzuki et al. Science 2019;365:377-381

Copyright © 2019, American Association for the Advancement of Science

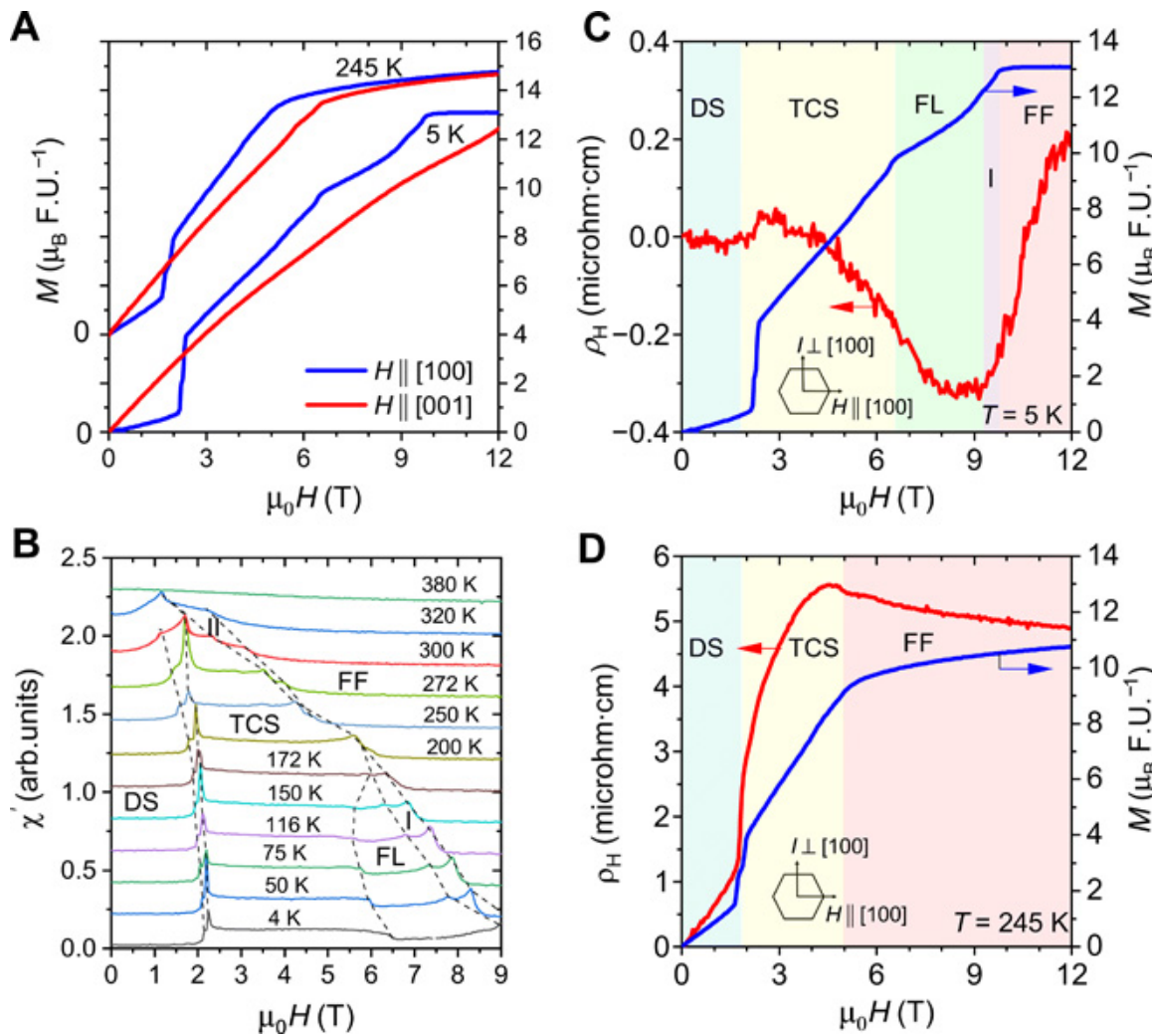
Science
AAAS

Magnetic Topological Properties in YMn₆Sn₆



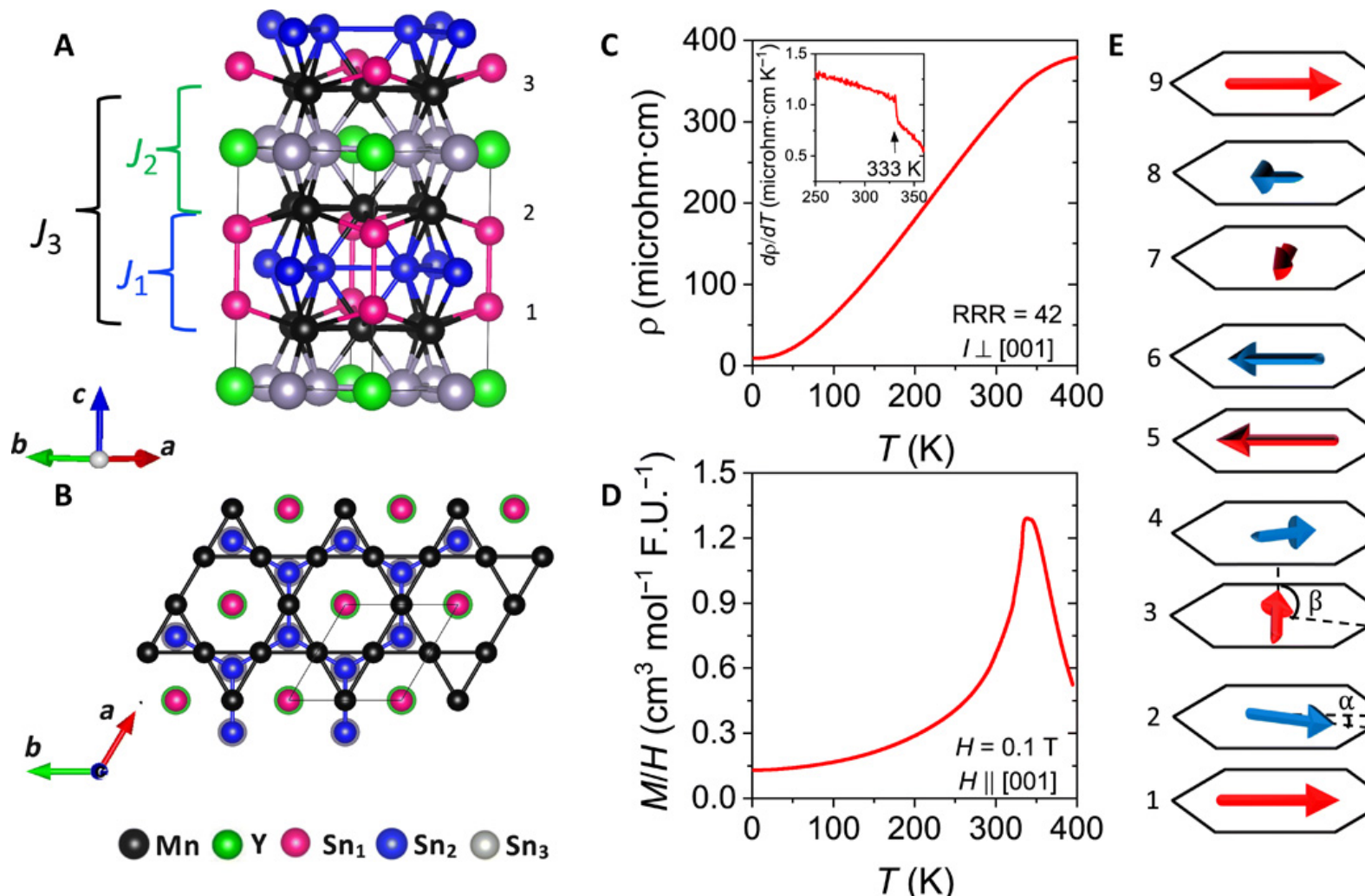
- Competing magnetic states and fluctuation-driven scalar spin chirality in the kagome metal YMn₆Sn₆, **Nirmal J. Ghimire, Rebecca L. Dally, L. Poudel, D. C. Jones, D. Michel, N. Thapa Magar, M. Bleuel, Michael A. McGuire, J. S. Jiang, John F. Mitchell, Jeffrey W. Lynn, and I. I. Mazin**, Science Advances **6**, eabe2680 (2020).
- Chiral properties of the zero-field spiral state and field-induced magnetic phases of the itinerant kagome metal YMn₆Sn₆, **Rebecca L. Dally, Jeffrey W. Lynn, Nirmal J. Ghimire, Dina Michel, Peter Siegfried, and Igor I. Mazin**, Phys. Rev. B **103**, 094413 (2021).

Fig. 2 Magnetization and Hall effect of YMn₆Sn₆.



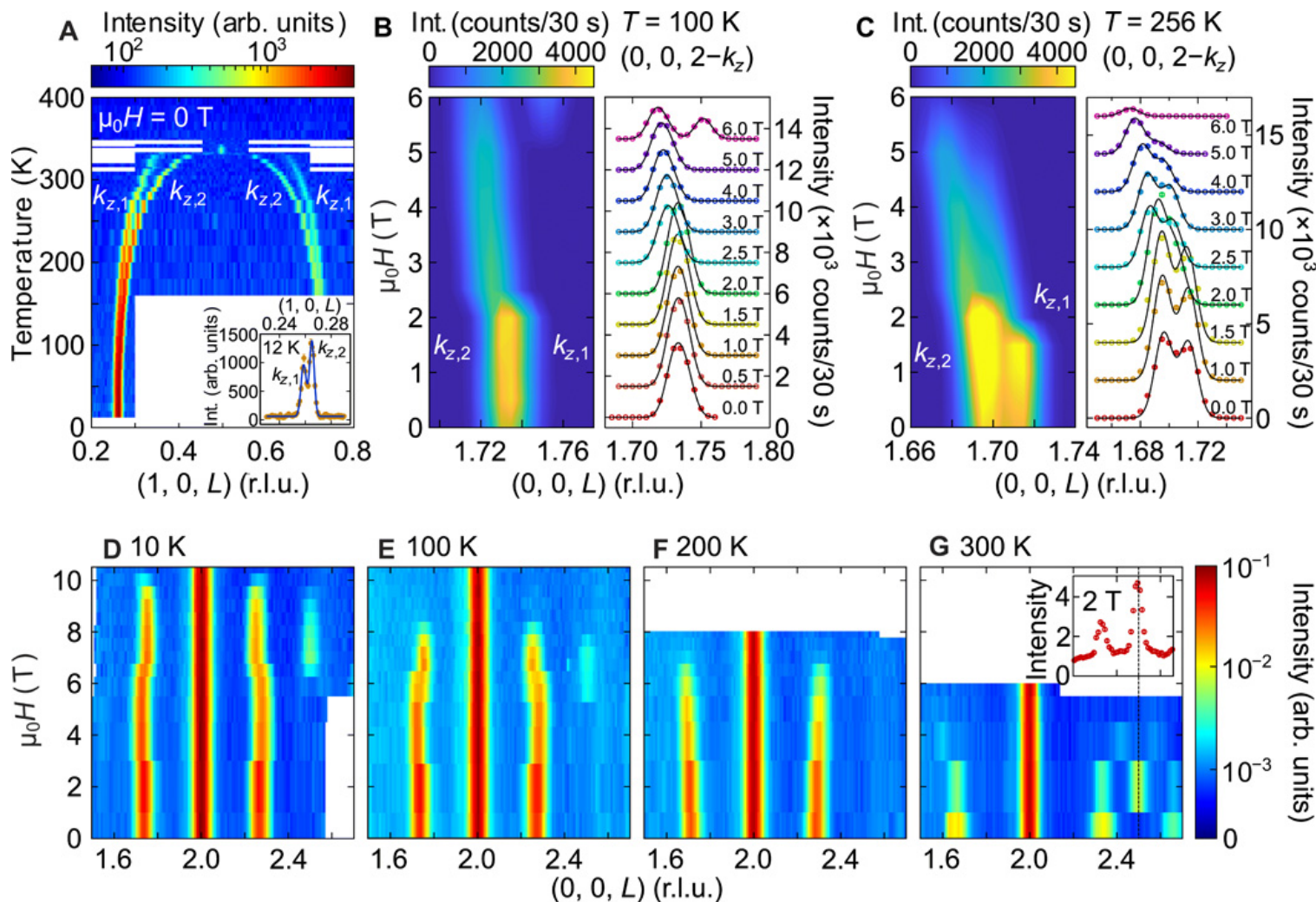
Nirmal J. Ghimire et al. Sci Adv 2020;6:eabe2680

Fig. 1 Crystal structure and electrical and magnetic properties of YMn₆Sn₆.



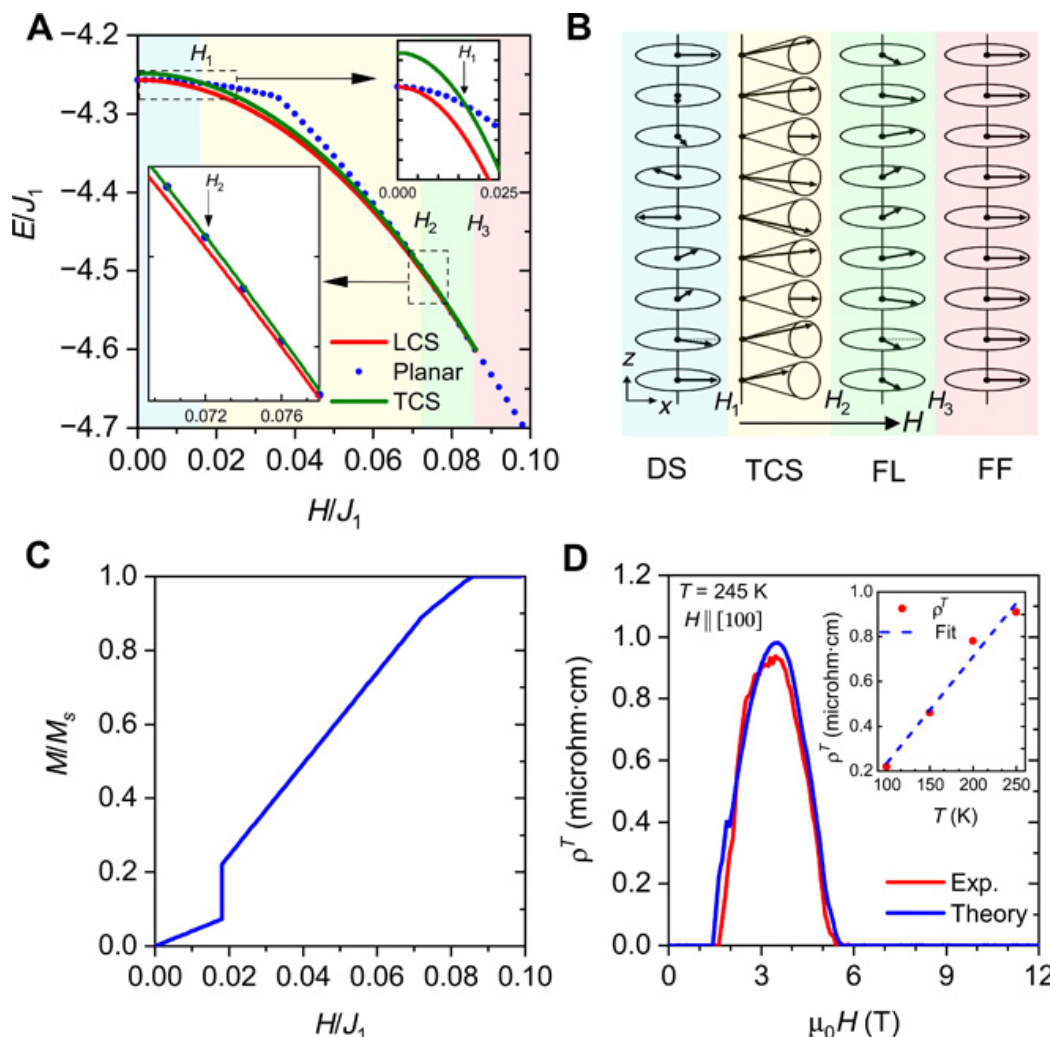
Nirmal J. Ghimire et al. Sci Adv 2020;6:eabe2680

Fig. 3 Single-crystal neutron diffraction of YMn₆Sn₆.



Nirmal J. Ghimire et al. Sci Adv 2020;6:eabe2680

Fig. 4 First-principles calculation and phenomenological model of spin chirality for THE.



Nirmal J. Ghimire et al. Sci Adv 2020;6:eabe2680

Summary

- Neutron scattering is a powerful tool investigate crystal and magnetic structures, and lattice and magnetic excitations, over six orders of magnitude in length scale and energy scale.
- Neutron and X-ray scattering are complementary experimental tools.
- National user facilities are available on a proposal basis to everyone.

References:

S. W. Lovesey, Theory of neutron scattering from condensed matter, Oxford: Clarendon Press - Oxford, 1984.

E. Balcar and S. Lovesey, Theory of Magnetic Neutron and Photon Scattering, Oxford: Clarendon Press, 1989.

L. Ament, M. van Veenendaal, T. P. Devereaux, J. P. Hill and J. van den Brink, "Resonant inelastic s-ray scattering studies of elementary excitations," *Rev. Mod. Phys.*, vol. 83, p. 705, 2011.

G. E. Bacon, Neutron Diffraction, Third ed., Oxford: Oxford University Press, 1975.

Magnetic Scattering, J. W. Lynn and B. Keimer, in *Handbook of Magnetism and Magnetic Materials*, ed. by Michael Coey and Stuart Parkin, (Springer Nature's Major Reference Work), (in press)

Neutron Nuclear Properties:

<https://www.ncnr.nist.gov/resources/n-lengths/>

<https://www.ncnr.nist.gov/instruments/magik/Periodic.html>

Magnetic Form Factors

<https://www.ill.eu/sites/ccsl/ffacts/ffachtml.html>

JWL website: <https://www.nist.gov/people/jeffrey-w-lynn>